JST

Journal homepage: http://penerbit.uthm.edu.my/ojs/index.php/jst
ISSN : 2229-8460 e-ISSN : 2600-7924

Journal of Science and Technology

On New Mathematical Modeling Measuring the Band Gap of Semiconductor in Nanomaterial

Aisha Salem*

Physics Department, Faculty of Science, Taibah University, Yanbu, Saudi Arabia

*Corresponding author

DOI: https://doi.org/10.30880/jst.2020.12.01.006
Received 12 February 2020; Accepted 23 June 2020; Available online 29 June 2020

Abstract: The magnitude and character components (M&C) band gap energy of semiconductor composite nanomaterial (SCN) is framed in this effort. The theoretical preparations supported by the energy increased by spacing the atoms in a crystalline state (solid energy) of the nano crystals compared to the bulk crystals. CdTe, CdSe, ZnSe, ZnTe and ZnS semiconductor composites were deliberated for the investigation of M&C components band gap dynamism. In addition, an entropy definition was employed in terms of this energy. It is confirmed that the band gap (BG) energy of SCN is subjected to the atom magnitude and character. From the layout, it can be concluded that the band gap energy increases whenever the atomic magnitude of the semiconductor nanomaterial reducing. The results attained were associated with the obtainable experimental information, which sustain the ability of the layout described.

Keywords: Mathematical modeling, Band gap, Semiconductor, Nanomaterial.

1. Introduction

Semiconductor nanomaterial is speedily growing field of scientific investigation for its unique optical, electrical, mechanical and photonic properties [1-10]. Recently, Hassan et al. [11] described the organizational, mechanical electronic, optical and magnetic performances in $Zn_{1-x}Mn_xS$ for ($0 \leq x \leq 1$), which calculated by utilizing Wein2K program. Some of these properties associated to the surface area to capacity fraction of the nanomaterial, which show a significant part to describe its properties. One of the principal and essential properties of semiconductors are their band gap (BG). BGs shows a central character in optical and electrical properties of semiconductor materials. Therefore, it is important to investigate the BGs growth of the semiconductor composite nanomaterial (SCN) to recognize the improved method of their properties. Semiconductor has wide demands in line for the wide BG. Bulk silicon is limited in practice due to its incidental and narrow BGs, whereas Si photon nano devices are extensively formed and utilized. Many experimental and theoretical researchers performed magnitude and character components (M&C) technique. The diameter requirement of the operative BGs in the nanowires are computed from photoluminescence spectra and equated to the investigational results aimed at InAs quantum bars and points to the calculations of numerous abstract systems [12].

Barnard [13] employed the electronic construction models to illustrate the character of single diamond nano crystals, which can deal with the BGs via the quantum control rule. In view of the quantum control results, holes and electrons in the semiconductors in nano scale are restrained. Consequently, the energy changes among the filled conditions and the unfilled positions growths or extending the BGs of the semiconductor [14]. Now for optoelectronics strategies, this larger BGs are extremely modifying the optical and electronic features of semiconductors at nano scale [15]. More experimentation achieved to measure the size of BGs via X-ray photoluminescence and photoemission spectroscopy [16-18]. However, the abstract estimate for the BG of SCN has its individual potentials. In addition,

*Corresponding author: ensalem@taibahu.edu.sa

limited theoretical constructions acknowledged that the M&C BGs of semiconductors nanomaterial, which takes the analysis to compute the band gap in complete variety unrestricted of estimate, still needs.

Recently, Datta et. al. [19] clarified the operational, optical, magnetic and electrical possessions of $Cd_{0.8}Fe_{0.2}S$ which is deliberated as thinned magnetic semiconductor. $Cd_{0.8}Fe_{0.2}S$ materials were synthesized utilizing composites method. Muhuddin et. al. [20] regenerated crystalline CuS nanoparticles from remaining result of chemical bath deposition and then using them for paintable CEs. The approach excluded the underuse of CuS NPs in conventional chemical bath deposition and delivered a one-dimensional and economically feasible method to improve the efficiency of the electrodes from the renewed CuS NPs.

Jubu and Yam [21] presented micro- and nanostructures of gallium oxide on silicon substrate by the hydrogen-decrease chemical vapor deposition method. They examined the effect of synthesis period and progress ambient on the surface morphology, crystal structure and band gap of the full-fledged films by utilizing field emission scanning electron microscope, high resolution X-ray diffraction and UV-Vis spectrophotometer, even though fundamental arrangement was established by energy dispersive X-ray diffraction technique.

In this study, created by a solid energy of hypothetical construction that does not consume adaptable factors, M&C band gap energy of SCN is suggested. This study generalizes the completely solid energy of the nanomaterial such that it covers the study of the investigation. The theoretical prediction employed to the CdTe, CdSe, ZnSe, ZnTe and ZnS semiconductors composite nanomaterial in nanowire, spherical and nano films. It is indicated that the atom of the M&C can modify the BG energy of the SCN. The new structure estimates are compared with the obtainable experimental information. A worthy arrangement agrees the influence of the suggested technique throughout the magnitude variety.

2. Experimental Results

This section explains the combination of ZnSe, CdSe and $Zn_{0.5}Cd_{0.5}Se$ semiconductor nanoparticles by employing thermal decomposition method. Related method and analysis were used to conclude how the possessions such as phase formation, particle sizes, crystallinity and M&C properties, magnitude dissemination, and optical possessions of arranged pure ZnSe and CdSe semiconductor nanomaterial affected by changing zinc, cadmium and selenium composition and calcination temperatures.

2.1 ZnSe Nanoparticles

It is well known that for nanocrystals of powder sample, the peaks presented a contraction by comparison to bulk ZnSe. Furthermore, all the XRD designs display strong considerations and no suggestion of contamination peaks detected. The magnitudes of the crystallites conforming to different temperatures of calcination calculated under the Scherrer's equation $D = \frac{k\lambda}{\beta cos\theta}$, where D and k respectively denote the average crystallite magnitude and the atom properties. The obtained crystallite magnitudes related to the ZnSe nanoparticles combined with fluctuating calcination temperatures and selenium applications designated in Table 1. Clearly, from this data, it is confirmed that growth in calcination temperature and zinc nitrate concentration determined a growth in crystallite magnitude. The obtainable outcomes in Table 1 established the nano sized construction of the illustrations and highlighted the great consequence of the temperature to the attained magnitude. In addition, the X-ray diffraction (XRD) analysis presented that the ZnSe particle sizes increases where the average crystalline sizes differ between 22 to 35 nm in line for the increases of the hydrothermal period (see Fig.1). The melting and combining of adjacent atoms due to the higher thermal energy was probably aim for the increasing in atom magnitude in relative to increases in calcination temperature. There is reliability between the transmission electron microscopy (TEM) consequences and the XRD results. Furthermore, the consequences resolve with TEM analysis, where the general magnitude supply accredited to the combination of the smaller atoms, which are thermodynamically unbalanced in the results of their high external energy, which categories them very sensitive (see Fig. 2).

The TEM micrographs of ZnSe nanoparticles synthesized over thermal treatment and exposed by calcination at temperatures of 450, 500, 600 and 700°C with 0.2 g selenium concentration exemplified in Fig. 2(a-d). Notwithstanding completing establishment, the ZnSe nanoparticles were not noticeable and showed a heterogeneous character delivery as shown in Fig. 2 (a) and (b). The growth in calcination temperature to 700°C resulted in substantial combination of various atoms. Consequently, the nanoparticles developed increasingly larger and attained transparency as in Fig. 2 (c) and (d).

Table 1 - Ordinary crystallite size of ZnSe nanoparticles exposed to changing calcination temperatures and selenium applications

Computation Temperature (°C)	0.2 g selenium Average size (nm)	0.4 g selenium Average size (nm)	0.6 g selenium Average size (nm)
450	10.5	12.0	14.2
500	12.0	13.8	16.0
600	16.0	18.0	19.0
700	20.0	23.0	24.0

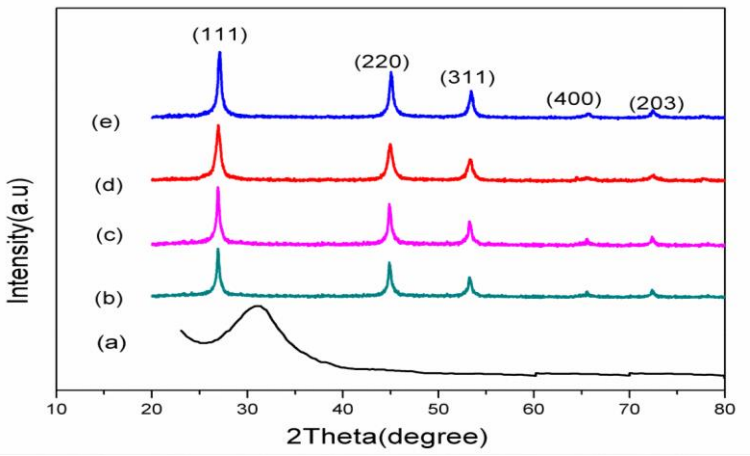

Fig. 1 - XRD peaks of ZnSe nanoparticles at 0.2 g selenium and varying calcination temperatures of (a) room temperature (b) 450 (c) 500 (d) 600 and (e) 700°C.

The synthesis of CdSe nanoparticles realized based on an aqueous result involving of cadmium nitrate, selenium in diverse applications 0.2, 0.4 and 0.6 g and the covering atom constancy and reduced aggregation. The TEM pictures in Fig. 4 (a-d) shows the homogeneity of the morphology and sizes supply of the models of CdSe nanoparticles exposed to calcination at diverse temperatures (450, 500, 600 and 700°C) and synthesized with 0.2 g selenium over thermal treatment. Depend on the XRD analysis, the TEM pictures exhibited that at 500°C the homogeneous spherical crystallites creating up the CdSe nanoparticles had a magnitude of 8 nm, despite the fact at 600°C they consumed a sizes of 13.5 nm. Moreover, the TEM consequences focus on the presence of straight proportionality between increase in atomic magnitude and growth in calcination temperature, the minimum magnitude actuality related with a calcination temperature of 500°C.

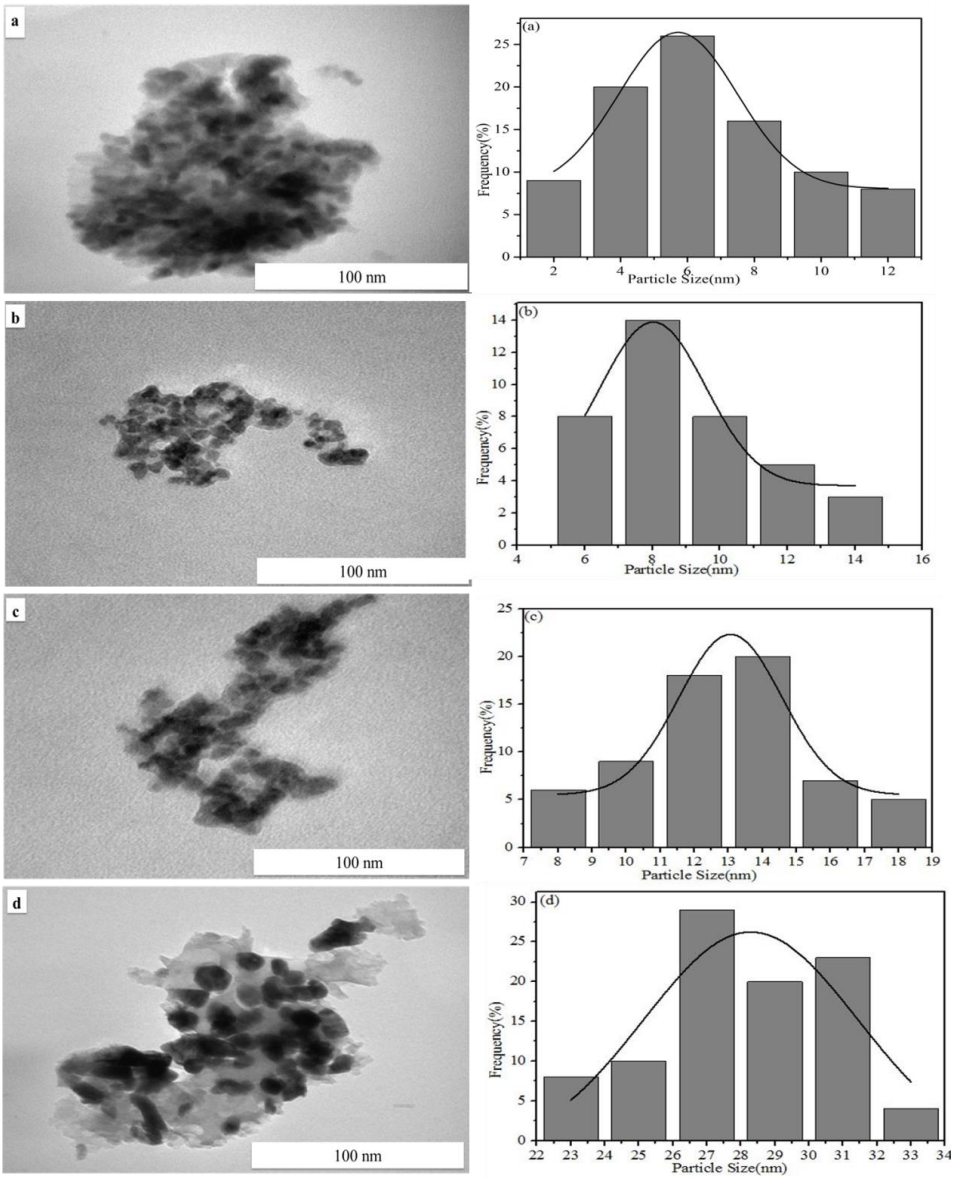

Fig. 2 - TEM images showing particle size distribution of CdSe nanoparticles synthesized at 0.2 g selenium and different calcination temperatures (a) 450°C (b) 500°C (c) 600°C and (d) 700°C.

3. Theoretical constructions

The complete solid energy of the nanomaterial can be viewed as a combination of the energy in line for the assistances of the interior particles and the surface particles. In [22], the formula presented as follows:

$$\Sigma_{total} = (n-N)\Sigma_0 + \frac{N}{2}\ \Sigma_0\ , \tag{1}$$

where *N* is the total value of surface particles and *n* is the total value of nano crystals. Consequently, (*n* −*N*) is the entire value of interiors particles in the nanomaterial. Σ_0 is the solid energy of the substance (bulk) material per particle. For the reason that the significance of melting thermo-dynamic factors of nano crystals on their powered, chemical and physical behaviors, the hidden heat of nano crystals function ƒ(δ) with the diameter δ has monotonous drops whenever δ decreases (see [23]). As a normal reflection, the function ƒ(δ) is correspondingly appropriate for the purpose of $\Sigma_0$function if the consistent evolution entropy concept for the solid–vapor evolution $\Xi = \int d\text{ƒ}(\delta)/\tau$ (τ is the bulk solid–vapor evolution temperature) utilized auxiliary. In virtue of this deliberation, Σ_0 function can deliver by the formal

$$\frac{\Sigma_0(\delta)}{\Sigma_0} = \left(1 - \frac{1}{\frac{\delta}{\delta_0}-1}\right)\left(e^{-\frac{2\Xi/\rho}{\frac{\delta}{\delta_0}-1}}\right), \tag{2}$$

where ρ is a constant of the ideal gas (in our simulation, we shall consider ρ~1) and δ_0 is the smallest diameter. From Eq. (1) we have

$$\frac{\Sigma_{total}(\delta)}{\Sigma_{total}} = (n-N)\frac{\Sigma_0(\delta)}{\Sigma_0} + \frac{1}{2}\ \frac{\Sigma_0(\delta)}{\Sigma_0}\ N. \tag{3}$$

Substituting (2) in (3) we get the general improved relation

$$\frac{\Sigma_{total}(\delta)}{\Sigma_{total}} = (n-N)\left(1 - \frac{1}{\frac{\delta}{\delta_0}-1}\right)e^{-\frac{2\Xi/\rho}{\frac{\delta}{\delta_0}-1}} + \frac{N}{2}\ \frac{\Sigma_0(\delta)}{\Sigma_0}e^{-\frac{2\Xi/\rho}{\frac{\delta}{\delta_0}-1}}. \tag{4}$$

Dividing Eq. (4) by *n* and denoting by $\Sigma_n(\delta) = \frac{\Sigma_{total}(\delta)}{\Sigma_{total}}$ and $\Sigma_b(\delta) = \frac{\Sigma_0(\delta)}{\Sigma_0}$, we get the following total energy equation:

$$\Sigma_n(\delta) = \left(1 - \frac{N}{2n}\right)\left(\left(1 - \frac{1}{\frac{\delta}{\delta_0}-1}\right)e^{-\frac{2\Xi/\rho}{\frac{\delta}{\delta_0}-1}}\right)\Sigma_b(\delta)\ , \tag{5}$$

where Σ_b is the energy of bulk material. Consequently, by the construction of (5) we get the melting temperature (see [24])

$$\tau_n(\delta) = \left(1 - \frac{N}{2n}\right)\tau_b(\delta). \tag{6}$$

From (5) and (6), we get the relation between the melting temperature nanomaterial and the energy as follows:

$$\frac{\Sigma_n(\delta)}{\Sigma_b(\delta)} = \left(\left(1 - \frac{1}{\frac{\delta}{\delta_0}-1}\right)e^{-\frac{2\Xi/\rho}{\frac{\delta}{\delta_0}-1}}\right)\frac{\tau_n(\delta)}{\tau_b(\delta)}. \tag{7}$$

Hence, we arrive at the interesting relation, which describe the energy band gap

$$\Sigma_g(\delta) = \left(\left(1 - \frac{1}{\frac{\delta}{\delta_0} - 1} \right) e^{-\frac{2\Xi/\rho}{\frac{\delta}{\delta_0} - 1}} \right) \tau_g(\delta). \tag{8}$$

where $\Sigma_g(\delta) = \frac{\Sigma_n(\delta)}{\Sigma_b(\delta)}$ and $\tau_g(\delta) = \frac{\tau_n(\delta)}{\tau_b(\delta)}$ are the gap energy at temperature τ_g. In spherical shape, Eq. (8) becomes

$$\Sigma_g(\delta) = \left(\left(1 - \frac{1}{\frac{\delta}{\delta_0} - 1} \right) e^{-(\frac{2\Xi}{\rho})\frac{1}{\frac{\delta}{\delta_0} - 1}} \right) \left(1 + \frac{2\delta}{\Delta} \right), \tag{9}$$

Where δ is the diameter of a particle, and Δ is the diameter of the spherical Nano solids. In addition, for the nanowires equation recognizes in the following formula

$$\Sigma_g(\delta) = \left(\left(1 - \frac{1}{\frac{\delta}{\delta_0} - 1} \right) e^{-\frac{2\Xi/\rho}{\frac{\delta}{\delta_0} - 1}} \right) \left(1 + \frac{4\delta}{3\lambda} \right), \tag{10}$$

Where λ denotes the diameter of nanowire. Finally, the nano films represents in the next construction

$$\Sigma_g(\delta) = \left(\left(1 - \frac{1}{\frac{\delta}{\delta_0} - 1} \right) e^{-\frac{2\Xi/\rho}{\frac{\delta}{\delta_0} - 1}} \right) \left(1 + \frac{2\delta}{3\xi} \right), \tag{11}$$

where the character ξ indicates the width of the Nano film. Note that, the difference in Nano solids between the two states usually small, therefore, the value of entropy is negative. Moreover, the inverse of the compressibility knows as the bulk model.

4. Results and discussion

CdSe nanocrystals and growing CdTe cover of a wanted thickness. The CdSe/CdTe nanocrystals shaped presented a narrow PL band (≈ 27-35 nm) with quantum incomes as high as 50-85% at room temperature. Fluctuating production s perceived from green to red as the diameter of the CdSe cores increases. The photoconductivity of collections of 350 nm CdSe nanowires is considered by photosensitivity factors of 10–100 nm also, to ultrafast reply and rescue times of 20–40 μs with a thickness of 40 nm to form CdSe nanowire collection photodetector.

Nanomaterial analysis

Consider the following data in Table 2.

Table 2 - Effort factors

Nanomaterial	Σ_g [24]	δ	δ_0
CdSe	1.74	0.268	0.01
CdTe	1.44	0.286	0.01
ZnS	3.68	0.234	0.01
ZnSe	2.71	0.254	0.01
ZnTe	2.39	0.189	0.01

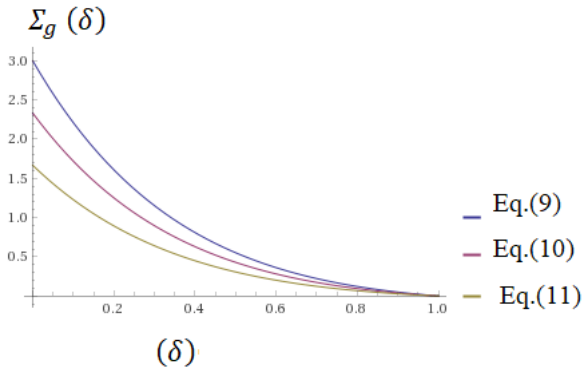

Fig. 3 - The energy band gap as given in Eq.s (9), (10) and (11).

The results confirmed that the band gap energy $\Sigma_g\ (\delta)$ rises with the lessening atom diameter. It is observed that when the atom magnitude (diameter δ) is less than 0.6, there is extensive increase in the rate of $\Sigma_g\ (\delta)$. Furthermore, the expected consequences are in arrangement with the current investigational information for the complete range of the nanomaterial. The proposed method agrees by the quantum captivity theory. Fig. 3 presents the energy band gap of nanomaterial in spherical nano solids, nanowire and nano films intended by Eqs (9)-(11), along with the experimental data [25, 26], which aid our model. As showed in Fig. 1, the $\Sigma_g\ (\delta)$ rises with the reduction in atom magnitude. We confirm that $\Sigma_g\ (\delta)$ growths rabidly to the reduction of size 0.4 onwards. Our consequences are very close to the value in Table 1. The results compared with the obtainable experimental comments [27]. There is a worthy consensus between our proposed method and investigations. The magnitude has dependency of $\Sigma_g\ (\delta)$ of nanomaterial in nanowire by utilizing Eq. (10). Therefore, the $\Sigma_g\ (\delta)$ views as a nano scale. This can clarify quantum mechanical as the atom magnitude influences the nano scale, the value of covering of orbitals or energy level reductions and the thickness of band gets thinner. This will effect a growth in energy band gap among the valence band and the transfer band. Such a style of the $\Sigma_g\ (\delta)$ in Nanomaterial with their corresponding bulk matches all recent experiments (see Fig. 4 for 3D graph of Eqs (9)-(11).

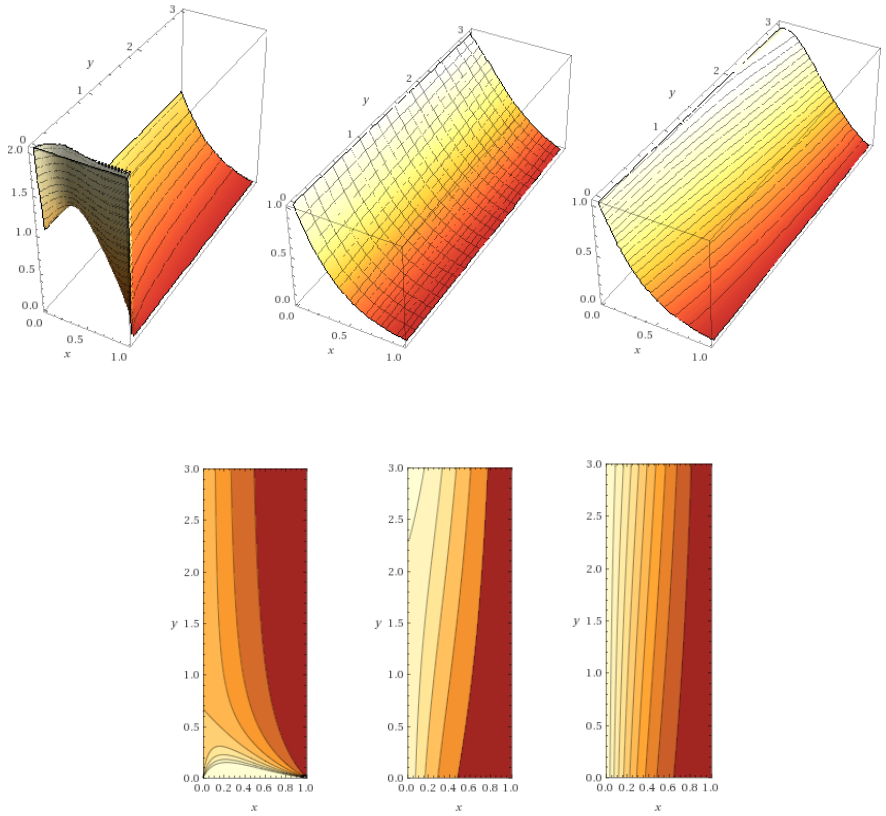

Fig. 4 - 3D graph and contours graph of Eqs (9)-(11), where y-axis represents to the length λ, Δ and ξ

Optical analysis

The optical $\Sigma_g\ (\delta)$ of the CdSe and ZnSe nanoparticles was assessed over the Tauc equation formulated by [26]:

$$(\omega h\mu)^{1/n} = \beta\ (h\mu - \Sigma_g\ (\delta)\ )^2 \qquad (12)$$

where ω represents the absorption constant, $h\mu$ is the photon energy of the occurrence light, $\Sigma_g\ (\delta)$ is the band gap energy, β is a constant and *n = 0.5, 1, 1.5* and *2* for qualified direct, permitted indirect, banned direct and banned indirect, correspondingly. The interest band gap of arranged examples was assessed by inferring the linear share of $(\omega h\mu)^2$ as a utility of hμ. Therefore, the seize of the generalized line on the x-axis specifies the $\Sigma_g\ (\delta)$ of the model. The tenets of $(\omega h\mu)^2$ versus (hμ) were schemed utilizing UV-Visible spectra of tasters demonstrated in Fig. 5 to regulate the optical tenets of the CdSe and ZnSe nanoparticles.

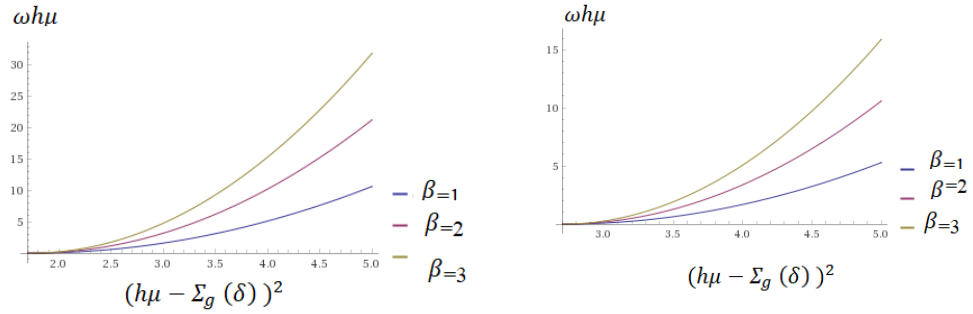

Fig. 5 - Optical band gap energy for CdSe & ZnSe nanoparticles respectively for β=1,2,3

Consequences display that the magnitudes of the found $\Sigma_g\ (\delta)$ for both CdSe and ZnSe nanoparticles are greater than the band gap energy for their bulk complements of 1.74 and 2.7 eV (see Table 2), correspondingly. It has been estimated that for CdSe is approximated to 1.9 and for ZnSe is 2.9 eV.

5. Conclusion

In transitory, a method expressed to compute the band gap energy ($\Sigma_g\ (\delta)$) of semiconductor nanomaterial for diverse magnitudes and characters, via spherical nano sphere, nanowires and nano films. It stated from the principle that $\Sigma_g\ (\delta)$ growths as atom magnitude of the semiconductor nanomaterial reductions. Additionally, our method estimates the $\Sigma_g\ (\delta)$ reliable with the obtainable experimental information. We guaranteed that this model would show a significant properties where experimental information not offered in the future.

Acknowledgement

The author would like to express all thanks to the Taibah University for the financial aid and facilities support throughout this research activity.

References

[1] Sun CQ. (2003) Oxidation electronics: bond-band-barrier correlation and its applications. *Prog Mater Sci*. 48:521-685.

[2] Sapra S, Sarma DD. (2004) Evolution of the electronic structure with size in II-VI semiconductor nanocrystals. *Phys Rev B*. 69:125304.

[3] Sun CQ, Li S, Tay BK, et al. (2002) Upper limit of blue shift in the photoluminescence of CdSe and CdS nanosolids. *Acta Mater*. 50:4687–4693.
[4] Viswanatha R, Sapra S, Saha-Dasgupta T, et al. (2005) Electronic structure of and quantum size effect in III-V and II-VI semiconducting nanocrystals using a realistic tight binding approach. *Phys Rev B*. 72:045333.
[5] Singh M, Hlabana KK, Singhal S, et al. (2016) Grain-size effects on the thermal conductivity of nanosolids. *J Taibah Univ Sci.*10:375–380.
[6] Li M, Li JC, Jiang Q. (2010) Size-dependent band-gap and dielectric constant of Si nanocrystals. *Int J Mod Phys B*.24:2297–2301.
[7] Amelia SM, Lincheneau C, Silvi S, et al. (2012) Electrochemical properties of CdSe and CdTe quantum dots. Chem Soc Rev. 41:5728.
[8] Mehr A, Emami F. (2014) Effects of structural factors on filtering operation of photonic band gap air bridges with circular and square shape holes. *Optik*. 125:2625–2632.
[9] Segets D, Lucas JM, Taylor RNK, et al. (2012) Determination of the quantum dot band gap dependence on particle size from optical absorbance and transmission electron microscopy measurements. *Acs Nano*. 6:9021–9032.
[10] Hassan M, Younas S, Sher F, et al. (2017) Room temperature ferromagnetism in single-phase Zn_{1-x} Mn_xS diluted magnetic semiconductors fabricated by coprecipitation technique. *App Phys A.*;123:352. doi:10.1007/s00339-017-0975-5.
[11] Hassan M, Noor NA, Mahmood Q, et al. (2016) Investigation of ferromagnetic semiconducting and opto-electronic properties of Zn1−xMnxS ($0 \leqslant x \leqslant 1$) alloys: A DFT-mBJ approach. *Current App. Phys*.16:1473–1483.
[12] Wang FD, Yu H, Jeong SH, et al. (2008) The scaling of the effective band gaps in indium−arsenide quantum dots and wires. *Acs Nano*. 2:1903–1913.
[13] Barnard AS. (2009) Shape-dependent confinement of the nanodiamond band gap. *Cryst Growth Des*. 9:4860 – 4863.
[14] Smith AM, Nie S. (2010) Semiconductor nanocrystals: structure, properties, and band Gap engineering. *Acc Chem Res*. 43:190–200.
[15] Canham LT. (1990) Silicon quantum wire array fabrication by electrochemical and chemical dissolution of wafers. *Appl Phys Lett*. 57:1046–1048.
[16] Torimoto T, Kontani H, Shibutani Y, et al. (2001) Characterization of ultrasmall CdS nanoparticles prepared by the size-selective photoetching technique. *J Phys Chem B*. 105:6838–6845.
[17] Nanda J, Kuruvilla BA, Sarma DD. (1999) Photoelectron spectroscopic study of CdS nanocrystallites. *Phys Rev B.*;59:7473–7479.
[18] Rao CNR, Kulkami GU, Thomas PJ, et al. (2002) Size-dependent chemistry: properties of nanocrystals. *Chem Eur* J.;8:29.
[19] Datta, Joydeep, *et al*. (2019) Improvement of charge transport for hydrothermally synthesized $Cd_{0.8}Fe_{0.2}S$ over co-precipitation method: A comparative study of structural, optical and magnetic properties. *Materials Science in Semiconductor Processing*, 91, 133-145.
[20] Muhyuddin, Mohsin, et al. (2019) A new insight into solar paint concept: regeneration of CuS nanoparticles for paintable counter electrodes in QDSSCs. *Applied Physics A* 125.10 : 716.
[21] Jubu, Peverga Rex, and F. K. Yam. (2020) Influence of growth duration and nitrogen-ambient on the morphological and structural properties of beta-gallium oxide micro-and nanostructures. *Materials Chemistry and Physics*, 239 :122043.
[22] Qi WH. (2005) Size effect on melting temperature of nanosolids. *Physica B*.368:46–50.
[23] Rose JH, Ferrante J, Smith JR. (1981) Universal binding energy curves for metals and bimetallic interfaces. *Phys Rev Lett*. 47:675–678.
[24] Singh, Madan, Monika Goyal, and Kamal Devlal. (2018) Size and shape effects on the band gap of semiconductor compound nanomaterials. *Journal of Taibah University for Science*, 12.4, 470-475.
[25] Li LL, Hu J, Yang W. (2001) Band gap variation of size- and shape-controlled colloidal CdSe quantum rods. *Nano Lett*. 1:349–351.
[26] Li J, Wang LW. (2005) Band-structure-corrected local density approximation study of semiconductor quantum dots and wires. *Phys Rev B.*72:125325.
[27] Mastai Y, Hodes G. (1997) Size quantization in electrodeposited CdTe nanocrystalline films. *J Phys Chem B*. 101:2685–2690.